

# 1 **Orthogonal control of gene expression in plants using synthetic** 2 **promoters and CRISPR-based transcription factors**

3  
4 Shaunak Kar<sup>1,2,#</sup>, Yogendra Bordiya<sup>1,4,#</sup>, Nestor Rodriguez<sup>1</sup>, Junghyun Kim<sup>1</sup>, Elizabeth  
5 C. Gardner<sup>1,2</sup>, Jimmy Gollihar<sup>3</sup>, Sibum Sung<sup>1,\*</sup> and Andrew D. Ellington<sup>1,2,\*</sup>

6  
7  
8 <sup>1</sup> Department of Molecular Biosciences, University of Texas at Austin, Austin TX, USA

9 <sup>2</sup> Center for Systems and Synthetic Biology, University of Texas at Austin, Austin, TX,  
10 USA

11 <sup>3</sup> US Army Research Laboratories–South, Austin, Texas, USA

12 <sup>4</sup> Present address: Life Sciences Solutions group, Thermo Fisher Scientific, Austin, TX,  
13 USA

14  
15 # Authors contributed equally

16 \* Corresponding authors

17  
18 Sibum Sung: [sbsung@austin.utexas.edu](mailto:sbsung@austin.utexas.edu), Andrew D. Ellington: [ellingtonlab@gmail.com](mailto:ellingtonlab@gmail.com)

## 19 20 21 **Abstract**

22  
23 **Background:** The construction and application of synthetic genetic circuits is frequently  
24 improved if gene expression can be orthogonally controlled, relative to the host. In plants,  
25 orthogonality can be achieved via the use of CRISPR-based transcription factors that are  
26 programmed to act on natural or synthetic promoters. The construction of complex gene  
27 circuits can require multiple, orthogonal regulatory interactions, and this in turn requires  
28 that the full programmability of CRISPR elements be adapted to non-natural and non-  
29 standard promoters that have few constraints on their design. Therefore, we have  
30 developed synthetic promoter elements in which regions upstream of the minimal 35S  
31 CaMV promoter are designed from scratch to interact via programmed gRNAs with dCas9  
32 fusions that allow activation of gene expression.

34 **Results:** A panel of three, mutually orthogonal promoters that can be acted on by artificial  
35 gRNAs bound by CRISPR regulators were designed. Guide RNA expression targeting  
36 these promoters was in turn controlled by either Pol III (U6) or ethylene-inducible Pol II  
37 promoters, implementing for the first time a fully artificial Orthogonal Control System  
38 (OCS). Following demonstration of the complete orthogonality of the designs, the OCS  
39 was tied to cellular metabolism by putting gRNA expression under the control of an  
40 endogenous plant signaling molecule, ethylene. The ability to form complex circuitry was  
41 demonstrated via the ethylene-driven, ratiometric expression of fluorescent proteins in  
42 single plants.

43

44 **Conclusions:** The design of synthetic promoters is highly generalizable to large tracts  
45 of sequence space, allowing Orthogonal Control Systems of increasing complexity to  
46 potentially be generated at will. The ability to tie in several different basal features of  
47 plant molecular biology (Pol II and Pol III promoters, ethylene regulation) to the OCS  
48 demonstrates multiple opportunities for engineering at the system level. Moreover, given  
49 the fungibility of the core 35S CaMV promoter elements, the derived synthetic promoters  
50 can potentially be utilized across a variety of plant species.

51

52

### 53 **Keywords**

54 Synthetic transcription factor, orthogonal promoter, modular cloning, plant synthetic  
55 biology

56

## 57 **Introduction**

58

59 The field of synthetic biology aims to revolutionize biotechnology by rationally engineering  
60 living organisms (1-6). One aspect of rational engineering is to embed biological  
61 organisms with complex information processing systems that can be used to control  
62 phenotypes (2, 3, 7, 8), often via synthetic gene circuits that can predictably regulate  
63 and tune expression of endogenous as well as transgenes (4, 9-11).

64 However the performance of such synthetic genetic circuits is often plagued by unwanted  
65 interactions between the circuit components and the host regulatory system, which can  
66 lead to loss of circuit function (10). These unprogrammed interactions can be mitigated  
67 via the design and use of genetic parts that have minimal cross-talk with the host, creating  
68 orthogonal regulatory or orthogonal control systems (OCS) that can further serve as the  
69 basis for constructing complex genetic programs with predictable behaviors. In the last  
70 two decades an increasing number of well-characterized genetic parts have been  
71 combined in circuits capable of complex dynamic behaviors, including bi-stable switches,  
72 oscillators, pulse generators, Boolean-complete logic gates (7, 12-15). While OCS and  
73 the circuits that comprise them were initially characterized in microbial hosts, more  
74 recently a significant fraction of them have been constructed and characterized in  
75 eukaryotic hosts such as yeast and mammalian cells (12, 16-19). More recently, synthetic  
76 transcriptional control elements have begun to be characterized in plants (20-22).

77 While a variety of artificial plant transcription factors containing diverse DNA binding  
78 domains and plant-specific regulatory sequences are known (20, 22), orthogonal control  
79 requires more programmable DNA binding domains and modular regulatory domains (20,

80 22-24). To this end, we describe an alternate strategy for the construction of orthogonal  
81 transcriptional regulatory elements in plants, powered by a single universal transcriptional  
82 factor – dCas9:VP64 which has been shown to work in a wide variety of eukaryotic  
83 species, including plants (16, 25, 26). While this transcription factor has primarily been  
84 used for the regulation of endogenous genes (25-27), here we describe a generalizable  
85 strategy for the universal design and use of synthetic promoters that rely only on the  
86 production of specific gRNAs to program dCas9:VP64, and the use of this set of mutually  
87 orthogonal promoters for the bottom-up construction of circuits that show multiplexed  
88 control of gene expression.

89

#### 90 **Design of a modular cloning framework for facile construct assembly**

91

92 Traditionally the process of construction of these synthetic gene expression systems has  
93 relied on time-consuming practices of recombinant DNA technology like design of custom  
94 primers, PCR amplification, gel extraction of PCR products. Over the last decade the  
95 advent of high-throughput cloning techniques, such as Golden-gate cloning with Type IIS  
96 restriction enzymes, has greatly accelerated the design-build-test cycle for the  
97 construction and prototyping of synthetic circuits (7, 9, 28, 29). Because the overlaps for  
98 assemblies can be modularly specified, multiple parts can be assembled sequentially in  
99 a single tube reaction.

100 While a Golden-Gate framework was previously described for the construction of plant  
101 expression vectors (30), here we used the highly optimized modular cloning (MoClo)  
102 framework, instantiated as a yeast toolkit (YTK) as the basis of our architecture (28).

103 Recently, beyond yeast expression vectors, this framework has been adapted for the  
104 construction of a mammalian toolkit (MTK) (9). Along with both YTK and MTK, a plant  
105 toolkit based on the YTK architecture will prove essential for seamlessly porting parts and  
106 circuits across diverse eukaryotes. Briefly, in this framework the entire vector is divided  
107 into particular ‘part’ types flanked by Bsal restriction sites followed by a unique ligation  
108 site. Promoters, genes and terminators are generally categorized into Type 2, 3 and 4  
109 parts respectively where each part type has a unique overhang that dictates the  
110 compatibility between part types (9, 28) (**Fig 1A, S1A**). This preserves the architecture of  
111 each transcriptional unit (promoter-gene-terminator). For the assembly of multiple  
112 transcriptional units (TU), each transcriptional unit is first cloned into an ‘intermediate’  
113 vector flanked by connector sequences that dictate the order of the TUs to be stitched  
114 together. By using appropriate connectors, each TU can be further assembled into a final  
115 expression vector in a single pot reaction (**Fig S1B**) [20]. This modular approach enables  
116 rapid assembly of increasingly complex genetic circuits comprised of multiple  
117 transcriptional units.

118 Since *Agrobacterium*-based transformation has been the staple for plant genetic  
119 engineering for decades (31), we used compatible vectors as the basis for our framework,  
120 and designed and constructed three YTK-compatible shuttle vectors. Each expression  
121 vector contains the pVS1 replicon (an *Agrobacterium* origin of replication – OriV and two  
122 supporting proteins – RepA and StaA) and pBR22 origin for propagation in *Agrobacterium*  
123 and *E.coli* respectively, and a common antibiotic selection cassette (KanR) that has been  
124 shown to be functional in both species (**Fig 1B, Materials and Methods**) (29, 30). The  
125 three constructs otherwise differed in the plant selection marker - BASTA, hygromycin,

126 and kanamycin. The resistance markers were expressed from the Nos promoter and also  
127 contained a Nos terminator (30) (**Fig 1B**). The backbone also contains a GFP drop-out  
128 cassette that allows easy identification of correct assemblies, which should appear as  
129 colonies that lack fluorescence (9, 28) (**Fig 1B**).

130

131 Fluorescence and luminescence reporters are frequently used to study protein  
132 localization and interaction in plants and animals (32). To provide these useful reporter  
133 parts in the context of our system, we cloned the strong promoter from Cauliflower mosaic  
134 virus (35S) as a Type 2 part and its corresponding terminator as a Type 4 part (33, 34).  
135 These parts can be matched with a number of fluorescent reporter genes (GFP, BFP,  
136 YFP and RFP) all as Type 3 parts for robust reporter expression. Combinations of these  
137 proteins can also potentially be used for BIFC (Bimolecular Fluorescence  
138 Complementation) (35). Similarly, luciferase is commonly used in plant molecular biology  
139 to study circadian rhythm (36), test the spatiotemporal activities of regulatory elements  
140 (37), and to study the plant immune system (38, 39). Therefore we adapted a luciferase  
141 gene from *Photinus pyralis*, commonly known as firefly luciferase (F-luc) (21).

142

143 Single TUs comprised of a 35S promoter, fluorescent reporter genes and the luciferase  
144 gene, and a terminator that serves as a polyadenylation signal were assembled into the  
145 *Agrobacterium* shuttle expression vector (**Fig 2A-C**). The activity of constructs was  
146 assayed using transient expression in *Nicotiana benthamiana* (30). As expected, we see  
147 strong activity of the promoter with the expression of the respective reporter genes (**Fig**  
148 **2A-C**). In order to diversify the promoters used in circuits (and thereby avoid

149 recombination and potentially silencing), we also included a well-characterized promoter  
150 from the Ti plasmid that drives mannopine synthase (Pmas) (40-43). When the 35S  
151 promoter was swapped with Pmas, similar expression levels of YFP were achieved (**Fig**  
152 **2D**).

153

## 154 **Development of an Orthogonal Control System (OCS) to regulate transgene** 155 **expression**

156 One of the primary difficulties with using synthetic biology principles and methods to  
157 engineer organisms, especially in eukaryotes, is that the functionality of synthetic circuits  
158 is often plagued by unwanted interactions of the circuit ‘parts’ with the underlying  
159 regulatory machinery of the host (44). As a particularly relevant example, systems  
160 developed in the past for transgene expression caused severe growth and developmental  
161 defects in *Arabidopsis* and *Nicotiana benthamiana* (45, 46). Therefore, it is paramount to  
162 develop regulatory tools to control transgene expression that minimizes the impact on  
163 endogenous plant machinery/physiology, while maintaining the modularity and scalability  
164 of synthetic approaches in general.

165

166 A potential solution to this problem is to develop orthogonal ‘parts’ that of necessity  
167 function independently of endogenous regulation by the host. To this end, we set out to  
168 develop a fully integrated Orthogonal Control System (OCS) based on orthogonal  
169 synthetic promoters driven by an Artificial Transcription Factor (ATF). We started with  
170 the deactivated form of the Cas9 protein (dCas9) fused to the transcriptional activator  
171 domain VP64 as a highly programmable ATF (26, 27). While dCas9:VP64 has previously

172 been shown to upregulate the expression of endogenous genes via specific guide RNAs  
173 (gRNAs) that target the promoter region upstream of those genes (25, 47), this strategy  
174 has not been utilized for the construction of a fully orthogonal system in which custom  
175 promoters can be similarly regulated. Here we develop a suite of synthetic promoters  
176 (pATFs, promoter for Artificial Transcription Factor) in which each promoter has a similar  
177 modular architecture: varying number of repeats of gRNA binding sites followed by a  
178 minimal 35S promoter (33, 34). This system is inherently scalable, since new binding  
179 sites bound by new gRNAs can be built at will. The complete list of parts (promoters,  
180 genes and terminators) is provided in **Supplementary Table 1**.

181  
182 We initially varied the number of gRNA binding sites (3 and 4) upstream of the minimal  
183 35S promoter, and analyzed expression of the reporter using transient assay in *Nicotiana*  
184 *benthamiana*. Three repeats provided the best expression of the reporter gene without  
185 significant background (**Fig 3A**). The promoter architecture was further assayed for leaky  
186 expression by generating pATF:YFP/BFP/RFP constructs and expressing gRNA  
187 constitutively in the absence of dCas9:VP64 (**Fig 3A**). None of these constructs show  
188 expression above background (**Fig 3B and 3C**). However, upon the addition of  
189 constitutively expressed dCas9:VP64 cassette to the circuit, induction of reporter protein  
190 expression was observed (**Fig. 3B and 3C**). Each pATF demonstrated comparable levels  
191 of expression (pATF1:YFP - 3-fold, pATF3:BFP - 6-fold and pATF4:RFP - 2 fold)  
192 compared to that obtained from the regular 35S promoter (6-fold; **Fig 2B**). The basic  
193 features of the pATF and corresponding gRNAs can thus form the basis for the OCS and  
194 should allow us to predictably control reporter and other gene circuits. The complete list



195 of assembled OCS circuits is provided in **Supplementary Table 2**; as the reader will see,  
196 OCS circuitry can be organized in terms of increasing complexity and demonstrates how  
197 the Design-Built-Test approach can be used to empirically generate ever more  
198 substantive plant phenotypes.

199 In order to show that the OCS designs could also function in stable transgenic *Arabidopsis*  
200 *thaliana* lines, we assembled the OCS 1-1 and 4-1 circuits (**Supplementary Table 2**;  
201 constitutive YFP and luciferase expression, respectively) in an *Agrobacterium* expression  
202 vector containing with a kanamycin selectable marker as described previously. These  
203 OCS constructs were successfully transformed into *Arabidopsis thaliana* plants (**Fig 4A**).  
204 As expected, the OCS 1-1 T<sub>1</sub> plants exhibited constitutive YFP expression (**Fig 4B**) while  
205 the OCS 4-1 plants were imaged (as described in **Methods**) and the constitutive  
206 expression of luciferase was confirmed (**Fig 4C, 4D**). Thus, the modular circuits  
207 assembled function in two species, as infiltrates in *Nicotiana* and as transgenics in  
208 *Arabidopsis*.

209

## 210 **Inducible gene expression system via the OCS framework**

211

212 The ability to precisely regulate the activity of the transgenes/circuit components based  
213 on specific input stimuli is a key feature in programmable synthetic circuits (48, 49). In  
214 order to enable orthogonal control of induction, we designed gRNA expression cassettes  
215 to produce functional gRNAs from inducible Pol II promoters. To prevent nuclear export  
216 of gRNAs due to capping and polyadenylation, we used the hammerhead ribozyme  
217 (HHR) and Hepatitis Delta Virus (HDV) to cleave the 5' and the 3' ends of the gRNA,

218 respectively. This strategy has been previously shown to lead to the expression of  
219 functional gRNAs from Pol II promoters, with activity similar to those driven by the Pol III  
220 (U6) promoter (50).

221

222 To proof the ribozyme processed gRNA constructs, OCS circuits were assembled where  
223 gRNAs were either expressed from a U6 promoter (OCS 1-1) or the 35S promoter (OCS  
224 1-5), and could subsequently activate the transcription and expression of reporter genes  
225 (YFP) (**Fig 5A**). For both OCS circuits, downstream reporter gene expression was  
226 observed, at similar levels (**Fig. 5B**). The specific levels of gRNA obtained in each case  
227 were analyzed using qRT-PCR (**Fig 5C and 5D**), and as expected the level of gRNA from  
228 the strong Pol II (35S) driven expression was higher than those obtained with the U6  
229 promoter while similar levels of reporter expression were observed for both cases, thus  
230 demonstrating that this Pol II driven gRNA expression strategy can be effectively used for  
231 OCS activation (**Fig 5E**). For both these constructs the expression of hdCas9 (human  
232 codon optimized dCas9) was also confirmed via Western blot analysis (**Fig S2**).

233 In order to demonstrate that the Pol II-driven gRNAs could be used as part of an inducible  
234 OCS we used the well-characterized synthetic EBS promoter containing the EIN3 binding  
235 (51), and placed YFP under the downstream control of the ATF (via pATF-1) (**Fig 6A**).  
236 This circuit (OCS1-9) should be inducible by the volatile organic compound (VOC)  
237 ethylene, which is produced from its precursor ACC (1-aminocyclopropane-1-carboxylic  
238 acid). Time-dependent expression of YFP is observed in response to 10uM ACC  
239 induction (**Fig 6B**). Both the gRNA-1 and YFP expression levels were quantified before  
240 and after induction by qRT-PCR, a maximum of 3-fold induction was observed for both

241 cases (**Fig 6C and 6D**). Thus, this demonstrates that the activity from synthetic promoters  
242 can be controlled via the selective expression of the corresponding gRNAs.

243

### 244 **Construction of a panel of mutually orthogonal synthetic promoters**

245

246 Lack of multiplexed control of transgenes has been a major factor limiting the  
247 development of synthetic circuits in plants (5, 6). Multiplexed regulation in turn requires  
248 a panel of mutually orthogonal promoters and control elements that can operate  
249 simultaneously (5, 6). Our strategy for synthetic promoter design naturally leads to the  
250 generation of expression cassettes that are not only orthogonal to the host but are also  
251 mutually orthogonal. The degree of orthogonality can be tuned at will via the sequence  
252 design of the multiple gRNA components. By simply minimizing homology between  
253 gRNAs, we constructed two additional promoters similar to the architecture of pATF-1, in  
254 which gRNA binding sites were followed by a minimal 35S promoter (pATF-3 and pATF-  
255 4). The orthogonality of these promoters was assayed by assembling expression  
256 constructs in which each synthetic promoter controlled the production of a unique  
257 fluorescent reporter (pATF-1: YFP, pATF-3: RFP and pATF-4: BFP). The respective  
258 gRNAs (gRNA-1, gRNA-3 and gRNA-4) were separately transcribed from a U6 promoter  
259 (**Fig 7A**). When expression constructs were infiltrated into *Nicotiana benthamiana*, each  
260 of the synthetic promoters was specifically upregulated only when its corresponding  
261 gRNA was expressed; no background was detected from the remaining two synthetic  
262 promoters. (**Fig 7B and 7C**).

263

## 264 **Construction of complex ratiometric circuits**

265

266 Now that we have a suite of mutually orthogonal promoters, we sought to construct simple  
267 circuits where the activity of each promoter could be independently controlled. Three  
268 separate reporter proteins were used to simultaneously monitor the activity of two  
269 promoters: pATF-1 with YFP, while both RFP and BFP were under the control of the  
270 pATF-3. By leveraging the designed, orthogonal behavior of these promoters it proved  
271 possible to construct a ratiometric circuit wherein the activity of pATF-1, and hence YFP  
272 expression, was under the control of ethylene (via ACC), while pATF-3 constitutively  
273 drove the expression of RFP and BFP (**Fig 8A**). As expected, the addition of 10uM ACC,  
274 induced the expression of YFP from the pATF-1 promoter (3-fold), while the expression  
275 of the other reporters remained constant (**Fig 8B and 8C**). The ratiometric response was  
276 further validated by qRT-PCR; pATF-1 was induced 3-fold following a similar increase in  
277 expression of gRNA-1 while there were no changes observed in the transcription of the  
278 other two reporter genes (**Fig 8B and 8C**). The predictable behavior of the designed,  
279 artificial control elements in the ratiometric circuit is one of the first examples of complex  
280 circuitry to be described in plants, and demonstrates uniquely how natural metabolism  
281 and regulatory circuitry can be interfaced with free-standing orthogonal control systems.

282

283

## 284 **Discussion**

285

286 Transcriptional orthogonality is one of the bedrocks for circuit construction in synthetic  
287 biology, and generally serves as the basis for the bottom-up construction of complex  
288 circuitry for predictable dynamics (7, 10, 17). For eukaryotes the construction of multiple  
289 promoter elements is hindered by the typically complex regulatory sequences that lie  
290 upstream and within promoters (52-54).

291

292 The design of synthetic eukaryotic promoters has traditionally implemented a common  
293 architecture, where a strong transcriptional initiation region is cloned downstream of  
294 orthogonal DNA binding operator sequences and the latter serve as landing pads for  
295 synthetic transcription factors (23). The engineered transcription factors have typically  
296 consisted of DNA binding proteins (i.e., prokaryotic DNA binding proteins like TetR, LacI,  
297 LexA and PhIF (55-57)) fused to well characterized transcriptional activation domain like  
298 VP64. With the advent of programmable DNA binding proteins like zinc finger proteins  
299 and TALEs the repertoire of synthetic promoters greatly increased (23, 24, 58, 59). That  
300 said, each new synthetic promoter still requires the construction and characterization of  
301 its own unique transcription factor (23, 59, 60).

302

303 These bottlenecks can be circumvented by the use of the highly programmable RNA-  
304 guided DNA binding protein dCas9 (26). The dCas9 RNP fused to transcription activation  
305 domains such as VP64 has been used for the upregulation of endogenous genes in a  
306 wide variety of eukaryotic species like yeast, mammalian cells and plants (16, 25, 26,  
307 61). Here, we have used adapted this 'universal' transcription factor to control the  
308 expression of synthetic and orthogonal promoters without the need of addition of any

309 other factors. Using our modular framework, we were able to quickly design and  
310 characterize a panel of mutually orthogonal promoters that could drive the production of  
311 a variety of outputs, singly and in parallel, including different fluorescent proteins (GFP,  
312 BFP, RFP and YFP) and luciferase.

313

314 The activities of dCas9 based transcription factors can potentially be controlled by simply  
315 regulating the expression of their corresponding gRNAs (16, 17), enabling the coupling  
316 of natural and synthetic transcription units, and thus natural and overlaid metabolic  
317 responses. Here we have effectively used this strategy to couple ethylene sensing (via  
318 known EIN3 binding sites) to synthetic (pATF) promoters. Moreover, by changing the  
319 number and arrangement of gRNA binding sites synthetic promoters with different levels  
320 of activation can be generated, providing further opportunities for design (62). While it  
321 has been previously shown that a panel of minimal plant promoters can be used with  
322 natural DNA binding sequences for modulating promoter strengths (20), the addition of  
323 completely artificial, synthetic promoters as control elements should create opportunities  
324 for increasing the specificity and strengths of engineered promoters.

325 Since our strategy for designing synthetic promoters is generalizable it is likely that even  
326 more complex circuits can be built by simply incorporating other transcription factor  
327 binding sites, or by changing the regulatory 'headpiece' on the dCas9 element (for  
328 example, to a repressor), (63-65).

329

330 The stabilities of genetic circuitry in plants can be greatly modified by silencing and  
331 recombination, amongst other mechanisms (40, 41, 43). In this regard, the artificial

332 promoter elements that we generate can potentially be crafted to avoid repetition (20),  
333 and thus to better avoid silencing and recombination. As viable artificial promoter  
334 sequences continue to accumulate, they can be compared and contrasted to identify  
335 those that are least vulnerable to modification over time. The facile addition of new parts  
336 to the standardize toolkit architecture, particularly terminators, will further increase  
337 opportunities to avoid repetition in ways that again go well beyond what is possible by  
338 relying on just a few well-characterized endogenous elements alone.

339

340 The implementation of orthogonal control systems in plants can be used to limit cross-  
341 talk between natural and overlaid regulatory elements, allowing more precise response  
342 to a variety of inputs, from VOCs to hormones to temperature, water, and nutrients. The  
343 use of orthogonal control systems to enable more precise responses to pathogenesis is  
344 especially intriguing given the presence of R genes that are specifically responsive to  
345 individual pathogens (effector triggered immunity, ETI) (66). The architecture we have  
346 developed is fully generalizable, and can potentially be expanded to non-model plants  
347 and other eukaryotic species such as yeast and mammalian cells by the use of  
348 appropriate transcription initiation regions under the control of similar gRNA sequences  
349 binding sites (67).

350

## 351 **Materials and Methods**

352

### 353 ***Plasmid design and construction***

354

355 The plant expression vector was generated using the plasmid pICH86966  
356 (Addgene#48075) as the backbone. The lacZ expression cassette was replaced with the  
357 GFP dropout sequence (**Supplementary Table 2**) to make the plasmid compatible with  
358 YTK architecture design. All parts described in **Supplementary Table 1**, were cloned  
359 into the backbone pYTK001 (Addgene #65108). For the individual transcriptional units,  
360 the backbone used was pYTK095 (Addgene #65202) along with the appropriate  
361 connector sequences described in **Supplementary Table 3**. For the design of orthogonal  
362 gRNAs, random 20-mers were generated that had a GC content of ~50%, and that were  
363 at least 5 nucleotides away from all sequences in the *Nicotiana* and *Arabidopsis*  
364 genomes. All oligonucleotides and gblocks were obtained from Integrated DNA  
365 Technologies (IDT) unless otherwise stated.

366 For the construction of each genetic element namely promoters, coding sequences and  
367 terminators, first they were checked for restriction sites for the following enzymes –  
368 BsmBI, BsaI, NotI and DraIII. The restriction sites in the coding sequences were removed  
369 by the use of synonymous codons while the other elements did not contain any of these  
370 restriction sites. The complete list of parts and constructs are provided in **Supplementary**  
371 **Table 1**. The part plasmids were cloned into a common vector where each genetic  
372 element is flanked by BsaI restriction sites followed by appropriate overhangs  
373 (**Supplementary Table 1**). For the assembly of both single TU or multi-TU, the following  
374 procedure was used: 10 fmol of backbone plasmid and 20 fmol of parts/TUs were used  
375 in a 10uL reaction with 1ul of 10x T4 ligase buffer along with 100 units of BsaI-v2 (single  
376 TU) or Esp3I (multi-TU or parts) and 100 units of T7 DNA ligase. The cycling protocol  
377 used is: 24 cycles of 3 min at 37°C (for digestion) and 5 min at 16°C (for ligation) followed



378 by a final digestion step at 37°C for 30min and the enzymes were heat inactivated 80°C  
379 for 20 min. All constructs were transformed into DH10B cells, grown at 37°C using  
380 standard chemical transformation procedures. The colonies that lack fluorescence were  
381 inoculated and plasmids were extracted using Qiagen Miniprep kit according to the  
382 manufacturer's instructions Plasmids were maintained as the following antibiotics  
383 kanamycin (50ug/mL), chloramphenicol (34ug/mL) and carbenicillin (100ug/mL)  
384 wherever required. The plasmids were sequence verified by Sanger sequencing (UT  
385 Austin Genomic Sequencing and Analysis Facility). The correct constructs were then  
386 transformed into *Agrobacterium tumefaciens* strain GV3101 (resistant to Gentamycin and  
387 Rifampicin) and used either for transient expression in *Nicotiana benthamiana* or to  
388 generate stable lines in *Arabidopsis thaliana*. The following enzymes were used for the  
389 assemblies – Bsal-v2 (NEB #R3733S), Esp3I (NEB #R0734S) and T7 DNA ligase (NEB  
390 #M0318S).

391

### 392 ***Plant material, bacterial infiltration***

393 *Nicotiana benthamiana* and *Arabidopsis thaliana* plants were grown in soil at 22°C, and  
394 16 hr light period. For transient expression, three weeks old plants were syringe-infiltrated  
395 with *Agrobacterium tumefaciens* strain GV3101 (OD<sub>600</sub> = 0.5) and leaves were imaged  
396 under Olympus BX53 Digital Fluorescence Microscope or harvested for RNA and/or  
397 protein analysis. To create stable transformation in *Arabidopsis*, floral dip method (68)  
398 was used. T<sub>1</sub> plants were selected on half MS Kanamycin (50µg/ml) plates and the  
399 selected T<sub>1</sub> plants were analyzed using an Olympus BX53 Digital Fluorescence  
400 Microscope and a NightOwl imager for YFP expression and luciferase expression,

401 respectively. For circuits that constitutively expressed YFP (OCS1-1) and luciferase  
402 (OCS4-1) no other obvious phenotypic differences were observed across numerous  
403 individual plants.

404

#### 405 ***RNA extraction and qRT-PCR***

406 RNA was extracted using TRIzol reagent (Ambion). 1  $\mu$ g total RNA was used to synthesize  
407 cDNA. After DNaseI treatment to remove any DNA contamination, random primer mix  
408 (NEB #S1330S) and M-MLV Reverse transcriptase (Invitrogen #28025-013) were used  
409 for first strand synthesis. qRT-PCR was used to quantify the RNA prepared from transient  
410 expression experiments. AzuraQuant qPCR Master Mix (Azura Genomics) was used with  
411 initial incubation at 95 °C for 2 min followed by 40 cycles of 95 °C for 10 sec and 60 °C  
412 for 30sec. Level of target RNA was calculated from the difference of threshold cycle (Ct)  
413 values between reference (*5S rRNA*) and target gene using at least three independent  
414 replicates

415

#### 416 ***ACC treatment***

417 To check the induction of reporter in response to ACC in the plasmids containing  
418 pEBS::YFP/RFP/BFP, *Nicotiana benthamiana* leaves were infiltrated with Agrobacterium;  
419 after three days post infiltration, leaf discs were cut using cork borer and incubated in  
420 either 0  $\mu$ M or 10  $\mu$ M ACC for four hours. Fluorescence microscopy was used to check  
421 YFP expression after induction.

422

#### 423 **Fluorescence and Luminescence imaging**

424 Fluorescence microscope images after *Agrobacterium* mediated transient expression of  
425 YFP, BFP, RFP and GFP in *Nicotiana benthamiana* leaves were taken using an Olympus  
426 BX53 Digital Fluorescence Microscope. For this purpose, leaf discs were cut using cork  
427 borer from the area which was infiltrated. Images were taken using either 10X objective  
428 lens using the default filters for YFP (500/535nm), BFP (385/448nm), and RFP  
429 (560/630nm). The UV filter (350/460nm) was used to take GFP images. The exposure  
430 and gain setting were kept constant for each filter within each experiment to compare  
431 multiple leaf discs (3 to 6). In all the experiments a leaf disc from a leaf which was not  
432 infiltrated with *Agrobacterium* was used as a negative control in order to account for  
433 background fluorescence. All experiments were performed at least three times  
434 independently as indicated in the Results.

435 Expression of luciferase was detected using NightOwl II LB 983 *in vivo* imaging system  
436 ([https://www.berthold.com/en/bioanalytic/products/in-vivo-imaging-systems/nightowl-](https://www.berthold.com/en/bioanalytic/products/in-vivo-imaging-systems/nightowl-lb983/)  
437 [lb983/](https://www.berthold.com/en/bioanalytic/products/in-vivo-imaging-systems/nightowl-lb983/)). Leaves/plants were sprayed with 100 $\mu$ M D-luciferin, Potassium salt (GoldBio  
438 #LUCK-300). After 5 min of incubation, images were taken in the NightOwl II LB 983.  
439 Images were captured with a backlit NightOWL LB 983 NC 100 CCD camera. Photons  
440 emitted from luciferase were collected and integrated for a 2 min period. A pseudocolor  
441 luminescent image from blue (least intense) to red (most intense), representing the  
442 distribution of the detected photons emitted from active luciferase was generated using  
443 Indigo software (Berthold Technologies).

444

#### 445 **Western blot**

446 Total protein was extracted using urea-based denaturing buffer (100 mM NaH<sub>2</sub>PO<sub>4</sub>, 8 M

447 urea, and 10 mM Tris-HCl, pH 8.0) and used for immunoblot analysis to check the  
448 expression. The proteins were fractionated by 8% SDS-PAGE gel and transferred to a  
449 polyvinylidene difluoride (PVDF) membrane using a transfer apparatus according to the  
450 manufacturer's protocols (Bio-Rad). The membrane was treated with 5% nonfat milk in  
451 PBS-T for 10 min for blocking, and then incubated with Cas9 antibody (Santa cruz, 7A9-  
452 3A3, 1:500) at 4 °C for overnight. After incubation, the membrane was washed three times  
453 for 5 min and incubated with horseradish peroxidase-conjugated anti-mouse (1:10000)  
454 for 2 h. The Blot was washed with PBS-T three times and detected with the ECL system  
455 (Thermo scientific, lot# SE251206).

456

#### 457 **Declarations**

458

#### 459 **Ethics approval and consent to participate**

460 Not Applicable

461

#### 462 **Consent for publication**

463 Not Applicable

464

#### 465 **Availability of data and materials**

466

#### 467 **Competing interests**

468 The authors declare no competing interests.

469

470 **Funding**

471 This work was supported by the Defense Advanced Research Projects Agency (DARPA)  
472 agreement HR00111820048 to AE and SS. The content of the information does not  
473 necessarily reflect the position or the policy of the Government, and no official  
474 endorsement should be inferred. This work was also supported by Welch Foundation  
475 grant (F-1654) to ADE.

476

477 **Authors' contributions**

478 SK, SS and AE conceived of the project. SK designed the framework and the basic  
479 elements of OCS with input from EG, JG and SS. SK and YB assembled all constructs.  
480 YB, NR and JK performed all the testing in *Nicotiana* with input from SS. All authors  
481 contributed with the preparation of figures. SK, YB, JK, SS and AE wrote the manuscript  
482 with input from all authors.

483

484 **Acknowledgments**

485 We would also like to thank the Qiao lab (UT Austin) for providing details regarding the  
486 ethylene induction of the OCS constructs.

487

488 **Supplementary Information** includes

489

490 **Fig S1:** Workflow describing the assembly of single and multiple transcriptional units  
491 (TUs) in a plant expression vector; **Fig S2:** Western blot to analyze the expression of  
492 dCas9:VP64 in OCS constructs – OCS1-1 and OCS 1-5

493 **Table S1:** List of all genetic parts used for the construction of OCS constructs

494 **Table S2:** List of all OCS constructs

495 **Table S3:** List of all Addgene plasmids used in this work

496

497 **Full OCS plasmid maps**

498

## 499 **References**

500

- 501 1. Tolle F, Stucheli P, Fussenegger M. Genetic circuitry for personalized human cell therapy.  
502 *Current opinion in biotechnology*. 2019;59:31-8.
- 503 2. Scheller L, Fussenegger M. From synthetic biology to human therapy: engineered  
504 mammalian cells. *Current opinion in biotechnology*. 2019;58:108-16.
- 505 3. Sedlmayer F, Aubel D, Fussenegger M. Synthetic gene circuits for the detection,  
506 elimination and prevention of disease. *Nature biomedical engineering*. 2018;2(6):399-415.
- 507 4. Riglar DT, Silver PA. Engineering bacteria for diagnostic and therapeutic applications.  
508 *Nature reviews Microbiology*. 2018;16(4):214-25.
- 509 5. Kassaw TK, Donayre-Torres AJ, Antunes MS, Morey KJ, Medford JI. Engineering synthetic  
510 regulatory circuits in plants. *Plant science : an international journal of experimental plant biology*.  
511 2018;273:13-22.
- 512 6. de Lange O, Klavins E, Nemhauser J. Synthetic genetic circuits in crop plants. *Current*  
513 *opinion in biotechnology*. 2018;49:16-22.
- 514 7. Nielsen AA, Der BS, Shin J, Vaidyanathan P, Paralanov V, Strychalski EA, et al. Genetic  
515 circuit design automation. *Science (New York, NY)*. 2016;352(6281):aac7341.
- 516 8. Medford JI, Prasad A. Towards programmable plant genetic circuits. *The Plant journal :*  
517 *for cell and molecular biology*. 2016;87(1):139-48.
- 518 9. Fonseca JP, Bonny AR, Kumar GR, Ng AH, Town J, Wu QC, et al. A Toolkit for Rapid Modular  
519 Construction of Biological Circuits in Mammalian Cells. *ACS synthetic biology*. 2019;8(11):2593-  
520 606.
- 521 10. Brophy JA, Voigt CA. Principles of genetic circuit design. *Nature methods*. 2014;11(5):508-  
522 20.
- 523 11. Mutalik VK, Guimaraes JC, Cambray G, Lam C, Christoffersen MJ, Mai QA, et al. Precise  
524 and reliable gene expression via standard transcription and translation initiation elements.  
525 *Nature methods*. 2013;10(4):354-60.
- 526 12. Weinberg BH, Pham NTH, Caraballo LD, Lozanoski T, Engel A, Bhatia S, et al. Large-scale  
527 design of robust genetic circuits with multiple inputs and outputs for mammalian cells. *Nature*  
528 *biotechnology*. 2017;35(5):453-62.
- 529 13. Basu S, Gerchman Y, Collins CH, Arnold FH, Weiss R. A synthetic multicellular system for  
530 programmed pattern formation. *Nature*. 2005;434(7037):1130-4.
- 531 14. Gardner TS, Cantor CR, Collins JJ. Construction of a genetic toggle switch in *Escherichia*  
532 *coli*. *Nature*. 2000;403(6767):339-42.
- 533 15. Elowitz MB, Leibler S. A synthetic oscillatory network of transcriptional regulators.  
534 *Nature*. 2000;403(6767):335-8.
- 535 16. Kim H, Bojar D, Fussenegger M. A CRISPR/Cas9-based central processing unit to program  
536 complex logic computation in human cells. *Proceedings of the National Academy of Sciences of*  
537 *the United States of America*. 2019;116(15):7214-9.
- 538 17. Gander MW, Vrana JD, Voje WE, Carothers JM, Klavins E. Digital logic circuits in yeast with  
539 CRISPR-dCas9 NOR gates. *Nature communications*. 2017;8:15459.
- 540 18. Weber W, Fussenegger M. Engineering of synthetic mammalian gene networks.  
541 *Chemistry & biology*. 2009;16(3):287-97.

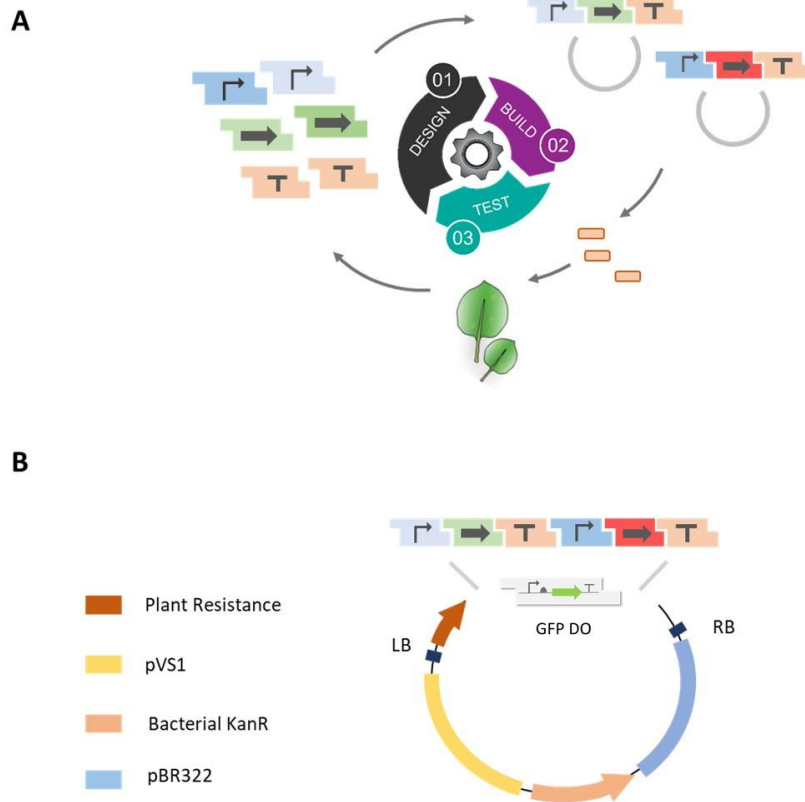
- 542 19. Kramer BP, Fussenegger M. Hysteresis in a synthetic mammalian gene network.  
543 Proceedings of the National Academy of Sciences of the United States of America.  
544 2005;102(27):9517-22.
- 545 20. Belcher MS, Vuu KM, Zhou A, Mansoori N, Agosto Ramos A, Thompson MG, et al. Design  
546 of orthogonal regulatory systems for modulating gene expression in plants. *Nature chemical*  
547 *biology*. 2020;16(8):857-65.
- 548 21. Schaumberg KA, Antunes MS, Kassaw TK, Xu W, Zalewski CS, Medford JI, et al.  
549 Quantitative characterization of genetic parts and circuits for plant synthetic biology. *Nature*  
550 *methods*. 2016;13(1):94-100.
- 551 22. Brückner K, Schäfer P, Weber E, Grützner R, Marillonnet S, Tissier A. A library of synthetic  
552 transcription activator-like effector-activated promoters for coordinated orthogonal  
553 gene expression in plants. *The Plant journal : for cell and molecular biology*. 2015;82(4):707-16.
- 554 23. Khalil AS, Lu TK, Bashor CJ, Ramirez CL, Pyenson NC, Joung JK, et al. A synthetic biology  
555 framework for programming eukaryotic transcription functions. *Cell*. 2012;150(3):647-58.
- 556 24. Bae KH, Kwon YD, Shin HC, Hwang MS, Ryu EH, Park KS, et al. Human zinc fingers as  
557 building blocks in the construction of artificial transcription factors. *Nature biotechnology*.  
558 2003;21(3):275-80.
- 559 25. Li Z, Zhang D, Xiong X, Yan B, Xie W, Sheen J, et al. A potent Cas9-derived gene activator  
560 for plant and mammalian cells. *Nature plants*. 2017;3(12):930-6.
- 561 26. Perez-Pinera P, Kocak DD, Vockley CM, Adler AF, Kabadi AM, Polstein LR, et al. RNA-guided  
562 gene activation by CRISPR-Cas9-based transcription factors. *Nature methods*. 2013;10(10):973-  
563 6.
- 564 27. Chavez A, Tuttle M, Pruitt BW, Ewen-Campen B, Chari R, Ter-Ovanesyan D, et al.  
565 Comparison of Cas9 activators in multiple species. *Nature methods*. 2016;13(7):563-7.
- 566 28. Lee ME, DeLoache WC, Cervantes B, Dueber JE. A Highly Characterized Yeast Toolkit for  
567 Modular, Multipart Assembly. *ACS synthetic biology*. 2015;4(9):975-86.
- 568 29. Engler C, Youles M, Gruetzner R, Ehnert TM, Werner S, Jones JD, et al. A golden gate  
569 modular cloning toolbox for plants. *ACS synthetic biology*. 2014;3(11):839-43.
- 570 30. Weber E, Engler C, Gruetzner R, Werner S, Marillonnet S. A modular cloning system for  
571 standardized assembly of multigene constructs. *PLoS one*. 2011;6(2):e16765.
- 572 31. Banta LM, Montenegro M. *Agrobacterium and Plant Biotechnology*. In: Tzfira T, Citovsky  
573 V, editors. *Agrobacterium: From Biology to Biotechnology*. New York, NY: Springer New York;  
574 2008. p. 73-147.
- 575 32. Berg RH, Beachy RN. Fluorescent protein applications in plants. *Methods Cell Biol*.  
576 2008;85:153-77.
- 577 33. Benfey PN, Chua NH. The Cauliflower Mosaic Virus 35S Promoter: Combinatorial  
578 Regulation of Transcription in Plants. *Science (New York, NY)*. 1990;250(4983):959-66.
- 579 34. Odell JT, Nagy F, Chua NH. Identification of DNA sequences required for activity of the  
580 cauliflower mosaic virus 35S promoter. *Nature*. 1985;313(6005):810-2.
- 581 35. Kerppola TK. Bimolecular Fluorescence Complementation (BiFC) Analysis as a Probe of  
582 Protein Interactions in Living Cells. *Annual Review of Biophysics*. 2008;37(1):465-87.
- 583 36. Tindall AJ, Waller J, Greenwood M, Gould PD, Hartwell J, Hall A. A comparison of high-  
584 throughput techniques for assaying circadian rhythms in plants. *Plant Methods*. 2015;11(1):32.



- 585 37. Xiong TC, Sanchez F, Briat J-F, Gaymard F, Dubos C. Spatio-Temporal Imaging of Promoter  
586 Activity in Intact Plant Tissues. In: Hehl R, editor. *Plant Synthetic Promoters: Methods and*  
587 *Protocols*. New York, NY: Springer New York; 2016. p. 103-10.
- 588 38. Xu G, Greene GH, Yoo H, Liu L, Marqués J, Motley J, et al. Global translational  
589 reprogramming is a fundamental layer of immune regulation in plants. *Nature*.  
590 2017;545(7655):487-90.
- 591 39. Zhou M, Wang W, Karapetyan S, Mwimba M, Marqués J, Buchler NE, et al. Redox rhythm  
592 reinforces the circadian clock to gate immune response. *Nature*. 2015;523:472.
- 593 40. Vaillant I, Schubert I, Tourmente S, Mathieu O. MOM1 mediates DNA-methylation-  
594 independent silencing of repetitive sequences in Arabidopsis. *EMBO Rep*. 2006;7(12):1273-8.
- 595 41. Matzke MA, Mette MF, Matzke AJ. Transgene silencing by the host genome defense:  
596 implications for the evolution of epigenetic control mechanisms in plants and vertebrates. *Plant*  
597 *Mol Biol*. 2000;43(2-3):401-15.
- 598 42. Ni M, Cui D, Einstein J, Narasimhulu S, Vergara CE, Gelvin SB. Strength and tissue  
599 specificity of chimeric promoters derived from the octopine and mannopine synthase genes. *The*  
600 *Plant Journal*. 1995;7(4):661-76.
- 601 43. Matzke MA, Primig M, Trnovsky J, Matzke AJ. Reversible methylation and inactivation of  
602 marker genes in sequentially transformed tobacco plants. *Embo j*. 1989;8(3):643-9.
- 603 44. Cardinale S, Arkin AP. Contextualizing context for synthetic biology – identifying causes of  
604 failure of synthetic biological systems. *Biotechnology Journal*. 2012;7(7):856-66.
- 605 45. Kang H-G, Fang Y, Singh KB. A glucocorticoid-inducible transcription system causes severe  
606 growth defects in Arabidopsis and induces defense-related genes. *The Plant Journal*.  
607 1999;20(1):127-33.
- 608 46. Amirsadeghi S, McDonald AE, Vanlerberghe GC. A glucocorticoid-inducible gene  
609 expression system can cause growth defects in tobacco. *Planta*. 2007;226(2):453-63.
- 610 47. Lowder LG, Paul JW, 3rd, Qi Y. Multiplexed Transcriptional Activation or Repression in  
611 Plants Using CRISPR-dCas9-Based Systems. *Methods in molecular biology* (Clifton, NJ).  
612 2017;1629:167-84.
- 613 48. Bayer TS, Smolke CD. Programmable ligand-controlled riboregulators of eukaryotic gene  
614 expression. *Nature Biotechnology*. 2005;23(3):337-43.
- 615 49. Kotula JW, Kerns SJ, Shaket LA, Siraj L, Collins JJ, Way JC, et al. Programmable bacteria  
616 detect and record an environmental signal in the mammalian gut. *Proceedings of the National*  
617 *Academy of Sciences*. 2014;111(13):4838.
- 618 50. Jacobs JZ, Ciccaglione KM, Tournier V, Zaratiegui M. Implementation of the CRISPR-Cas9  
619 system in fission yeast. *Nature Communications*. 2014;5(1):5344.
- 620 51. Cruz AB, Bianchetti RE, Alves FRR, Purgatto E, Peres LEP, Rossi M, et al. Light, Ethylene  
621 and Auxin Signaling Interaction Regulates Carotenoid Biosynthesis During Tomato Fruit Ripening.  
622 *Frontiers in Plant Science*. 2018;9(1370).
- 623 52. Lelli KM, Slattery M, Mann RS. Disentangling the many layers of eukaryotic transcriptional  
624 regulation. *Annual review of genetics*. 2012;46:43-68.
- 625 53. Ellwood K, Huang W, Johnson R, Carey M. Multiple layers of cooperativity regulate  
626 enhanceosome-responsive RNA polymerase II transcription complex assembly. *Mol Cell Biol*.  
627 1999;19(4):2613-23.

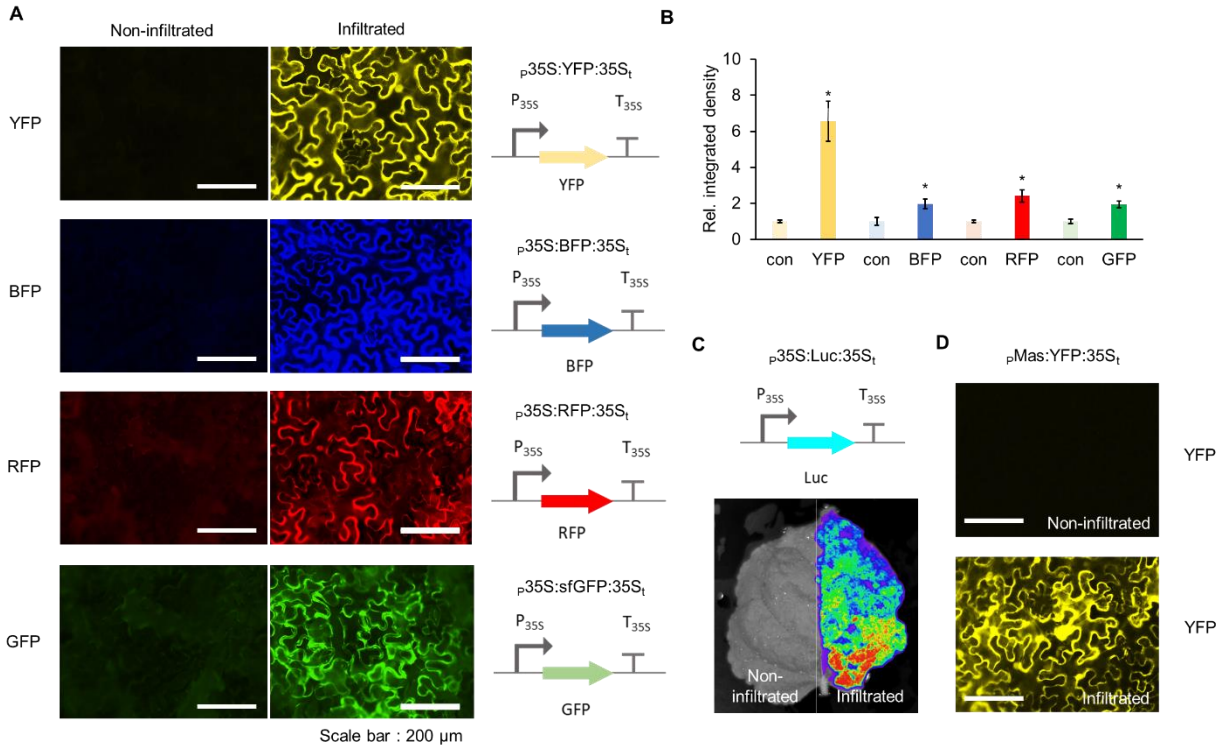


- 628 54. Chen L. Combinatorial gene regulation by eukaryotic transcription factors. *Curr Opin*  
629 *Struct Biol.* 1999;9(1):48-55.
- 630 55. Urlinger S, Baron U, Thellmann M, Hasan MT, Bujard H, Hillen W. Exploring the sequence  
631 space for tetracycline-dependent transcriptional activators: novel mutations yield expanded  
632 range and sensitivity. *Proceedings of the National Academy of Sciences of the United States of*  
633 *America.* 2000;97(14):7963-8.
- 634 56. Bellí G, Garí E, Piedrafita L, Aldea M, Herrero E. An activator/repressor dual system allows  
635 tight tetracycline-regulated gene expression in budding yeast. *Nucleic Acids Research.*  
636 1998;26(4):942-7.
- 637 57. Gossen M, Bujard H. Tight control of gene expression in mammalian cells by tetracycline-  
638 responsive promoters. *Proceedings of the National Academy of Sciences of the United States of*  
639 *America.* 1992;89(12):5547-51.
- 640 58. Perez-Pinera P, Ousterout DG, Brunger JM, Farin AM, Glass KA, Guilak F, et al. Synergistic  
641 and tunable human gene activation by combinations of synthetic transcription factors. *Nature*  
642 *methods.* 2013;10(3):239-42.
- 643 59. Li Y, Moore R, Guinn M, Bleris L. Transcription activator-like effector hybrids for  
644 conditional control and rewiring of chromosomal transgene expression. *Sci Rep.* 2012;2:897.
- 645 60. Cermak T, Doyle EL, Christian M, Wang L, Zhang Y, Schmidt C, et al. Efficient design and  
646 assembly of custom TALEN and other TAL effector-based constructs for DNA targeting. *Nucleic*  
647 *Acids Research.* 2011;39(12):e82.
- 648 61. Lowder LG, Zhang D, Baltes NJ, Paul JW, 3rd, Tang X, Zheng X, et al. A CRISPR/Cas9 Toolbox  
649 for Multiplexed Plant Genome Editing and Transcriptional Regulation. *Plant physiology.*  
650 2015;169(2):971-85.
- 651 62. Kocak DD, Josephs EA, Bhandarkar V, Adkar SS, Kwon JB, Gersbach CA. Increasing the  
652 specificity of CRISPR systems with engineered RNA secondary structures. *Nature biotechnology.*  
653 2019;37(6):657-66.
- 654 63. Pandelakis M, Delgado E, Ebrahimkhani MR. CRISPR-Based Synthetic Transcription  
655 Factors In Vivo: The Future of Therapeutic Cellular Programming. *Cell Syst.* 2020;10(1):1-14.
- 656 64. Yeo NC, Chavez A, Lance-Byrne A, Chan Y, Menn D, Milanova D, et al. An enhanced CRISPR  
657 repressor for targeted mammalian gene regulation. *Nature methods.* 2018;15(8):611-6.
- 658 65. Kwon DY, Zhao YT, Lamonica JM, Zhou Z. Locus-specific histone deacetylation using a  
659 synthetic CRISPR-Cas9-based HDAC. *Nature communications.* 2017;8:15315.
- 660 66. Gonzalez TL, Liang Y, Nguyen BN, Staskawicz BJ, Loqué D, Hammond MC. Tight regulation  
661 of plant immune responses by combining promoter and suicide exon elements. *Nucleic Acids*  
662 *Research.* 2015;43(14):7152-61.
- 663 67. Farzadfard F, Perli SD, Lu TK. Tunable and multifunctional eukaryotic transcription factors  
664 based on CRISPR/Cas. *ACS synthetic biology.* 2013;2(10):604-13.
- 665 68. Zhang X, Henriques R, Lin S-S, Niu Q-W, Chua N-H. Agrobacterium-mediated  
666 transformation of *Arabidopsis thaliana* using the floral dip method. *Nature Protocols.*  
667 2006;1(2):641-6.
- 668
- 669



670  
671  
672

673 **Figure 1. Schematic overview of the design-build-test cycle** **A.** Genetic elements  
674 such as promoters, genes and terminators are encoded as modular parts consisting of  
675 BsaI recognition sites flanked by specific overhangs to ensure the hierarchical assembly  
676 of transcriptional units. Once assembled, the constructs are transformed into  
677 *Agrobacterium* and the reporter expression is characterized in *Nicotiana benthamiana*  
678 leaf infiltrates **B.** Design of the shuttle vector backbone used for the assembly of  
679 constructs and subsequent propagation in *Agrobacterium*.



680

681

682 **Figure 2. Characterization of reporter constructs assembled using APT toolkit. A.**

683 Fluorescence microscope images showing *Agrobacterium* mediated transient expression

684 of YFP, BFP, RFP and GFP under the control of 35S promoter into *Nicotiana*

685 *benthamiana* leaves. Images on the left are from non-infiltrated leaves (negative control)

686 captured using the appropriate filter at same exposure and gain settings as was used for

687 the positive images on the right (**Material and Methods**). **B.** Relative integrated density

688 of each fluorescence signal (shown in panel A). Integrated density was measured using

689 image J software and normalized to that of a non-infiltrated control (con). Error bars: S.D.

690 (n=3, independent replicates). Asterisks indicate statistical significance in a student t-test

691 (P<0.05). **C.** Luminescence reporter luciferase expression shown by *Agrobacterium*

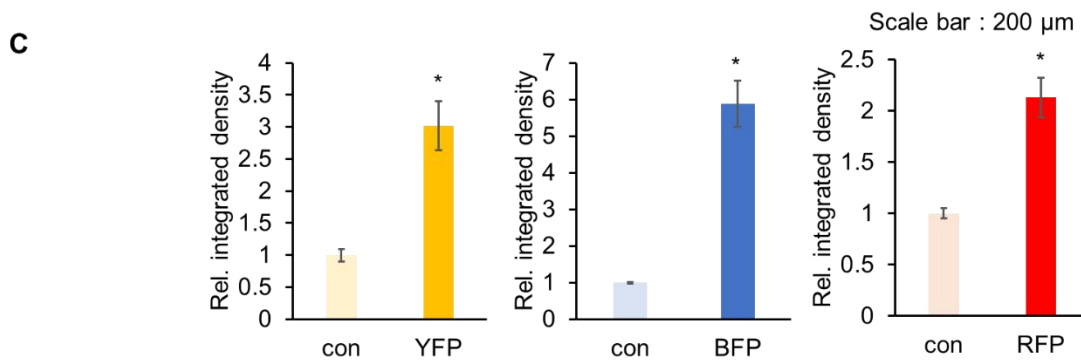
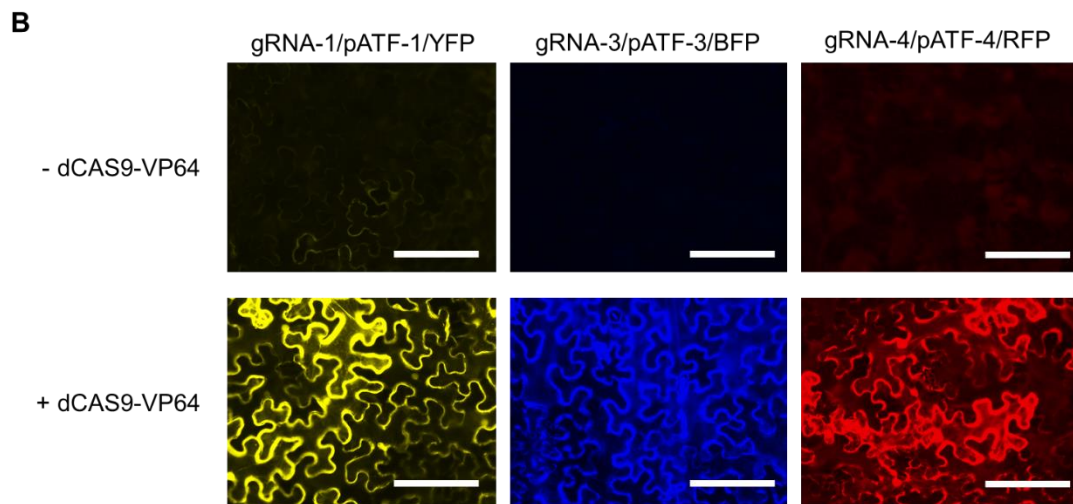
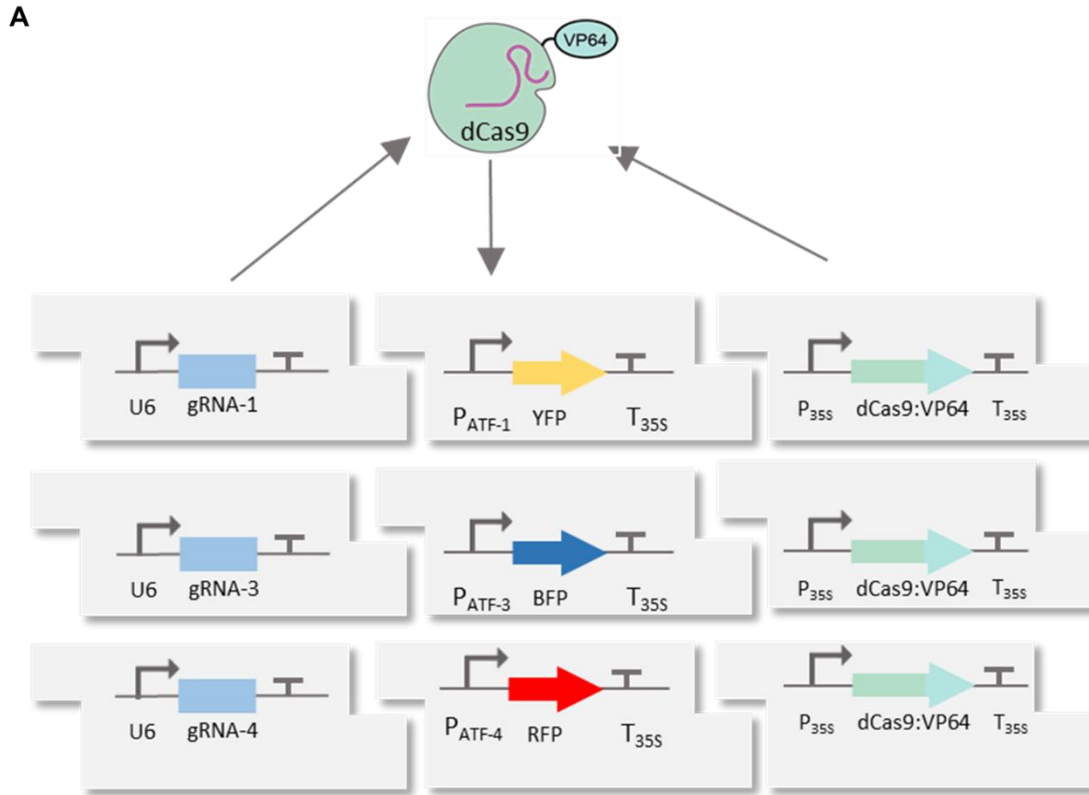
692 mediated transient expression of luciferase in *Nicotiana benthamiana* leaves. Left half of

693 the leaf was not infiltrated with *Agrobacterium*. **D.** Fluorescence microscope images

694 showing *Agrobacterium* mediated transient expression of YFP under MAS promoter in

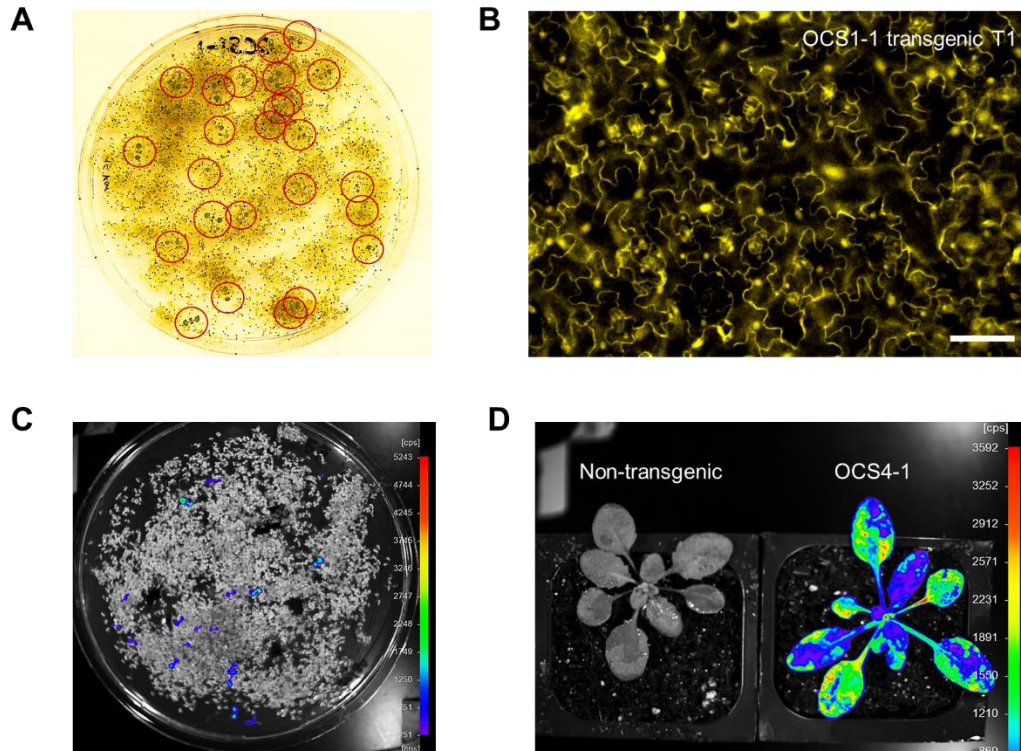
695 *Nicotiana benthamiana* leaves. Image on the left is the brightfield image for the same

696 construct.



697 **Figure 3. Characterization of activity of synthetic pATF promoters.** **A.** Circuit design  
698 of dCas9 based artificial transcription factor-controlled activation of synthetic promoters  
699 (pATFs). Specific *gRNAs* are produced by U6 promoter while the expression of the  
700 dCas9-VP64 is under the control of the 35S promoter. Reporter genes are under the  
701 control of the synthetic promoter (3 repeats of the *gRNA* followed by minimal 35S  
702 promoter to the artificial promoter (*gRNA* binding site) upstream of a specific fluorescence  
703 reporter. **B.** Fluorescence microscope image showing *Agrobacterium* mediated transient  
704 expression of YFP, BFP and RFP into *Nicotiana benthamiana* leaves with dCas9-VP64  
705 (bottom panels) and without dCas9-VP64 (upper panels) using three different *gRNAs*.  
706 Images were captured using the appropriate filter (Materials and Methods) at same  
707 exposure. **C.** Relative integrated density of each fluorescence signal (shown in panel B).  
708 Integrated density was measured using image J software and normalized to that of the  
709 control (con; - dCAS9-VP64). Error bars: S.D. (n=3, independent replicates). Asterisks  
710 indicate statistical significance in a student t-test ( $P < 0.05$ ).





711

712

713 **Figure 4. Evaluation of OCS reporter gene expression in transgenic *Arabidopsis***

714 **plants. A.** Image showing Kanamycin selection of the transgenic *Arabidopsis* seedlings

715 on MS media. Seedlings highlighted in the red circle have successfully incorporated OCS

716 circuit. Transformation efficiency is within reasonable ranges (~1%) determined by a

717 simple evaluation of the identified seedlings. **B.** Fluorescence microscope image of

718 *Arabidopsis* transgenic T<sub>1</sub> plants containing the constitutive expression of YFP under the

719 OCS control (OCS 1-1). Scale bar: 50 μm **C.** Image showing Kanamycin selection of the

720 transgenic *Arabidopsis* seedlings on MS media using luminescence reporter (OCS4-1)

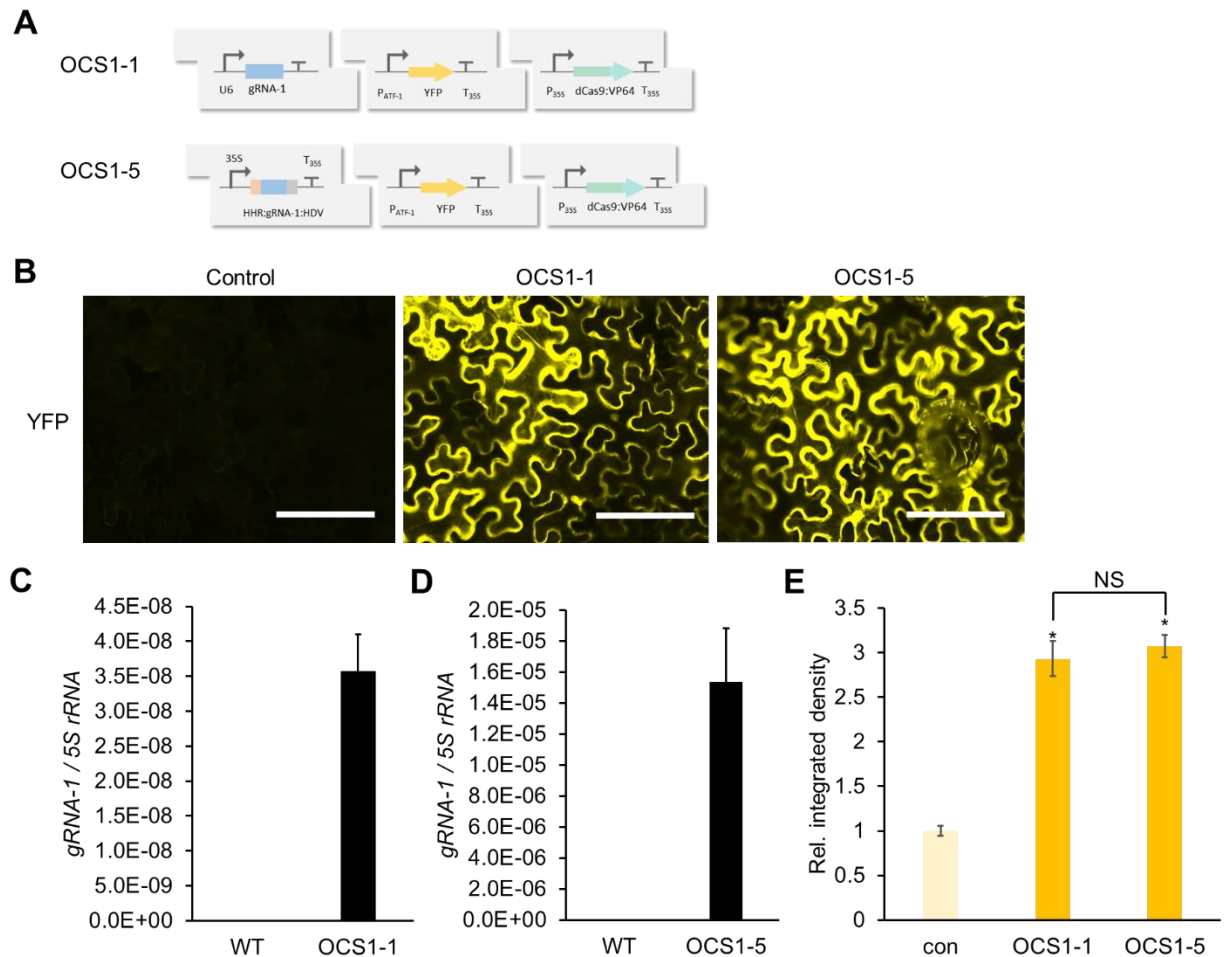
721 taken using the NightOwl (Methods). **D.** Image of a T<sub>1</sub> *Arabidopsis* plant containing OCS4-

722 1 at the rosette stage after spraying the luciferin (Methods) containing OCS4-1. This

723 image, taken at the rosette stage using NightOwl after luciferin spray, shows that the

724 luciferase expression is active throughout the adult plant. A non-transgenic plant on the

left was used as a negative control in the luminescence reporter assay.



725

726

727 **Figure 5. Design and characterization of gRNA expression modules under the**

728 **control of Pol II promoters. A.** OCS1-1 circuit generates RNA using U6 (Pol III) promoter

729 while OCS1-5 circuit generates gRNA using 35S (Pol II) promoter flanked by self-cleaving

730 ribozymes – HammerHead (HHR) and Hepatitis Delta Virus (HDV). **B.** Fluorescence

731 microscope images showing *Agrobacterium* mediated transient expression of OCS

732 constructs with two modalities of gRNA expression (OCS1-1 and OCS1-5). Control

733 images were taken without dCAS9-VP64 expression. Scale bars: 200  $\mu$ m **C** and **D.**

734 Quantification of the *gRNA-1* expression in OCS constructs (OCS 1-1 (C) and OCS 1-5

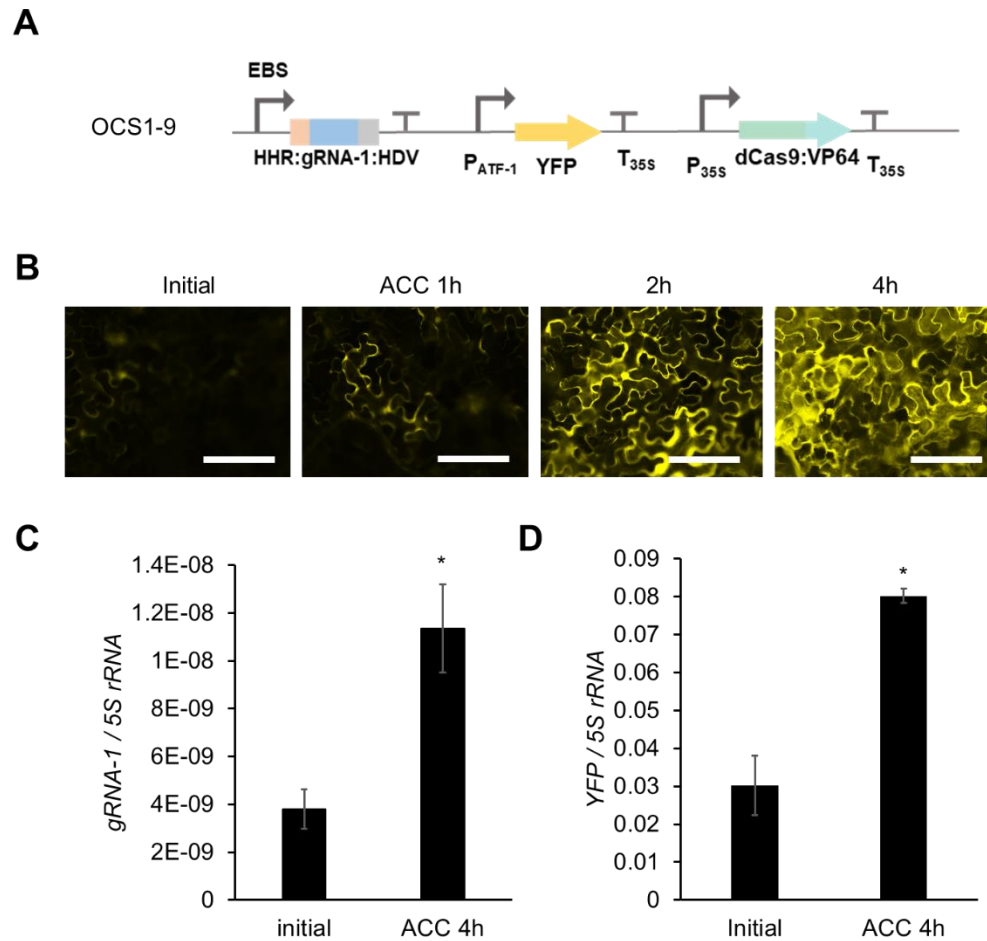
735 (D)) using qPCR relative to 5S *rRNA*. Error bars : S.D. (n=3, independent replicates) **E.**

736 Relative integrated density of each fluorescence signal (shown in panel B). Integrated

737 density was measured using image J software and normalized to that of the control (con;

738 - dCas9-VP64). Error bars: S.D. (n=3, independent replicates). Asterisks indicate

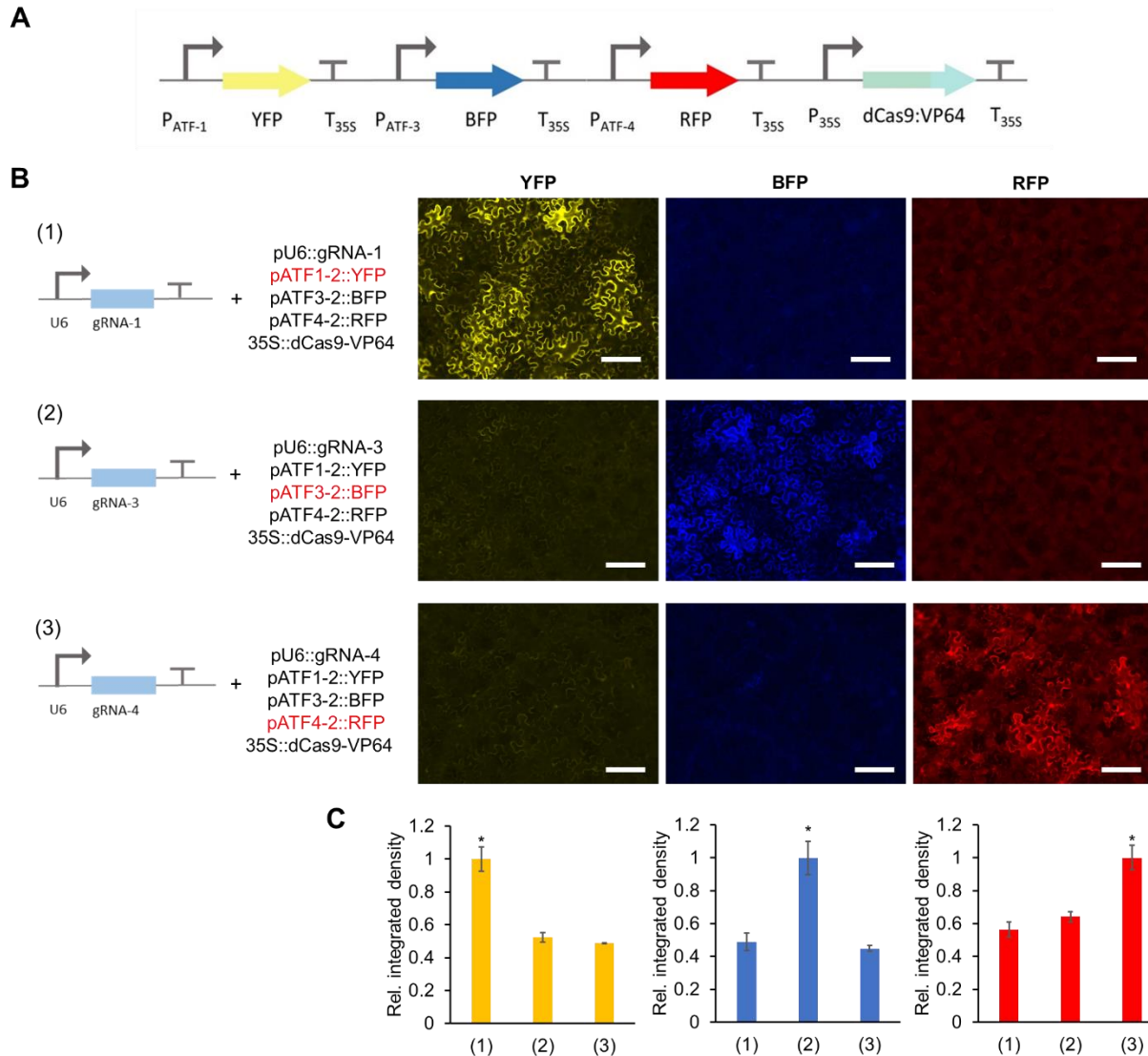
739 statistical significance in a student t-test ( $P < 0.05$ ). NS: not significant.



739

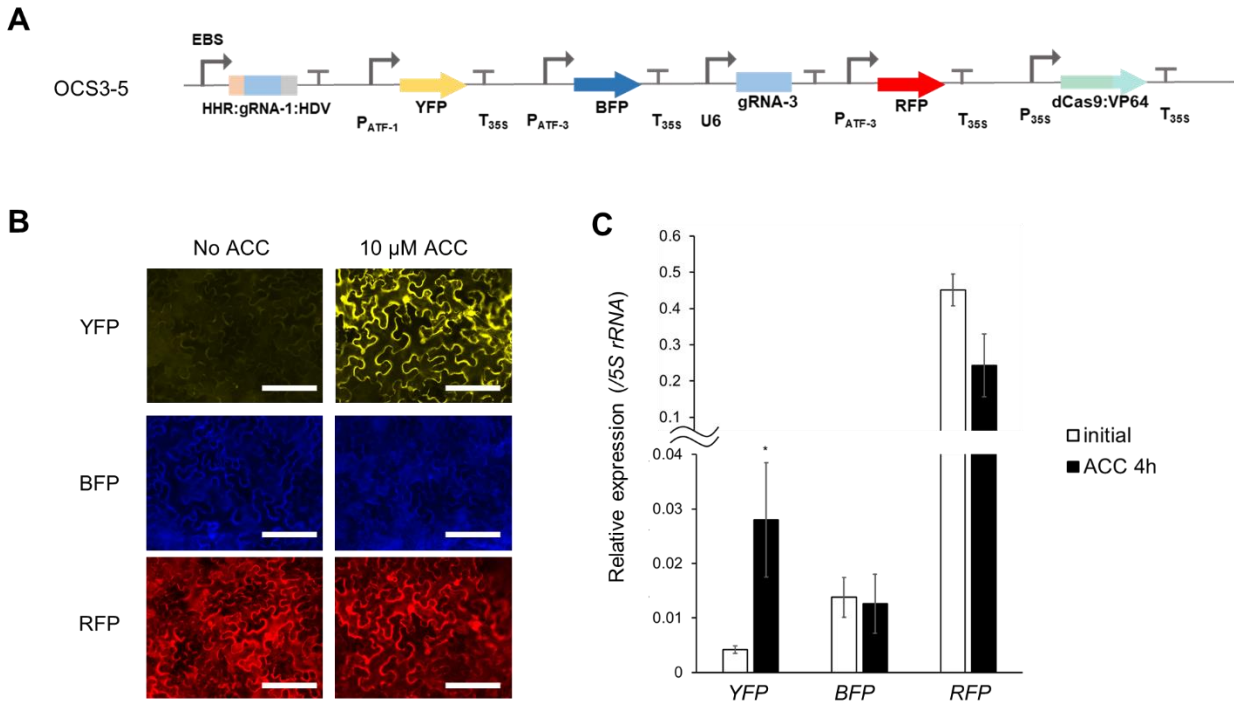
740 **Figure 6. Characterization of an ethylene inducible orthogonal control system. A.**  
741 OCS1-9 circuit (*gRNA-1* is expressed by ethylene inducible EBS promoter) **B.** Time  
742 course fluorescence microscope images showing *Agrobacterium* mediated transient  
743 expression of OCS1-9 in *Nicotiana benthamiana* leaves after induction with 10 $\mu$ M ACC.  
744 Scale bars: 200  $\mu$ m **C and D.** qPCR quantification of *gRNA-1* (C) and *YFP* (D) expression  
745 before and after induction with ACC, where both show similar levels of induction  
746 demonstrating that the relative change in *gRNA-1* expression (ethylene induction) results  
747 in the differential activation from the pATF-1 promoter. Error bars: S.D. (n=3, independent  
748 replicates), Asterisks indicate statistical significance in a student t-test (P<0.05).





749

750 **Figure 7. Degree of orthogonality of synthetic promoters.** **A.** OCS circuit containing  
751 all three synthetic promoters (pATF-1, pATF-3 and pATF-4) driving three different reporter  
752 genes namely YFP, BFP and RFP respectively with a single gRNA expressed one at a  
753 time under the control of U6 promoter. **B.** Fluorescence microscope images showing  
754 *Agrobacterium* mediated transient expression of OCS constructs in *Nicotiana*  
755 *benthamiana* leaves. Scale bars: 200  $\mu$ m **C.** As observed from the fluorescence images,  
756 only the specific gRNA:pATF pair is active, thus demonstrating that the synthetic  
757 promoters are mutually orthogonal. Relative integrated density of each fluorescence signal  
758 (shown in panel B). Integrated density was measured by image J software and normalized  
759 to the highest value. Error bars: S.D. (n=3, independent replicates). Asterisks indicate  
760 statistical significance in a student t-test (P<0.05).



761

762

763 **Figure 8. Design and characterization of a ratiometric circuit.** **A.** OSC3-5 contains

764 YFP which is inducible by ACC (pATF-1), while BFP and RFP are constitutively

765 expressed under the control of pATF-3 via the constitutive expression of gRNA-3. **B.**

766 Fluorescence microscope images showing *Agrobacterium* mediated transient expression

767 of the ratiometric OCS construct (OCS3-5) in *Nicotiana benthamiana* leaves with or

768 without 10 $\mu$ M ACC. Scale bars: 200  $\mu$ m **C.** qPCR quantification of YFP, BFP and RFP

769 shows that YFP is induced after the treatment with ACC while the expression of BFP and

770 RFP remains unchanged before or after ACC induction. Error bars: S.D. (n=4,

771 independent replicates). An asterisk indicates statistical significance in a student t-test (P

< 0.05).